A&A 460, 233–244 (2006)
DOI: 10.1051/0004-6361:20065035
© ESO 2006

Astronomy & Astrophysics

An explanation of the Z-track sources

M. J. Church[1,2], G. S. Halai[1], and M. Bałucińska-Church[1,2]

[1] School of Physics and Astronomy, University of Birmingham, Birmingham, B15 2TT, UK
e-mail: mjc@star.sr.bham.ac.uk
[2] Astronomical Observatory, Jagiellonian University, ul. Orla 171, 30-244 Cracow, Poland

Received 16 February 2006 / Accepted 4 September 2006

ABSTRACT

We present an explanation of the Z-track phenomenon based on spectral fitting results of *Rossi-XTE* observations of the source GX 340+0 using the emission model previously shown to describe the dipping Low Mass X-ray Binaries. In our Z-track model, the soft apex is a quiescent state of the source with lowest luminosity. Moving away from this point by ascending the normal branch the strongly increasing luminosity of the Accretion Disc Corona (ADC) Comptonized emission $L_{\rm ADC}$ provides substantial evidence for a large increase of mass accretion rate $\dot{M}$. There are major changes in the neutron star blackbody emission, kT increasing to high values, the blackbody radius $R_{\rm BB}$ decreasing, these changes continuing monotonically on both normal and horizontal branches. The blackbody flux increases by a factor of ten to three times the Eddington flux so that the physics of the horizontal branch is dominated by the high radiation pressure of the neutron star, which we propose disrupts the inner disc, and an increase of column density is detected. We further propose that the very strong radiation pressure is responsible for the launching of the jets detected in radio on the horizontal branch. On the flaring branch, we find that $L_{\rm ADC}$ is constant, suggesting no change in $\dot{M}$ so that flaring must consist of unstable nuclear burning. At the soft apex, the mass accretion rate per unit area on the neutron star $\dot{m}$ is minimum for the horizontal and normal branches and about equal to the theoretical upper limit for unstable burning. Thus it is possible that unstable burning begins as soon as the source arrives at this position, the onset of unstable burning being consistent with theory. The large increase in $R_{\rm BB}$ in flaring is reminiscent of radius expansion in X-ray bursts. Finally, in our model, $\dot{M}$ does not increase monotonically along the Z-track as often previously thought.

Key words. accretion: accretion disks – acceleration of particles – binaries: close – line: formation – stars: neutron – X-rays: binaries – X-rays: individuals: GX 340+0

1. Introduction

The Z-track sources form the brightest group of Low Mass X-ray Binary (LMXB) sources containing a neutron star, consisting of 6 members: GX 340+0, GX 5-1, Cyg X-2, Sco X-1, GX 17+2 and GX 349+2 (Hasinger & van der Klis 1989). All of these persistently radiate at about the Eddington limit for a neutron star and do not, in general, exhibit X-ray bursting characteristic of LMXBs with lower luminosities. The sources trace a Z-shaped pattern in X-ray hardness versus intensity or hardness versus softness demonstrating strong spectral evolution associated with major physical changes within the sources. However, the nature of these changes is not understood and this remains a significant astrophysical problem. Moreover, the Z-track sources are all detected as radio emitters showing relativistic jets to be present, but essentially on one branch only (e.g. Penninx 1989). The mechanism of jet formation also remains an important astrophysical problem. The occurrence of jets on one branch only may allow us to probe how jets are launched.

Hasinger et al. (1989) showed that the sources could be found on three different branches of a skewed Z-shape in a hardness-intensity diagram: the horizontal branch (HB), the normal branch (NB) and the flaring branch (FB). These diagrams demonstrated in a model-independent way that strong spectral evolution was taking place around the Z-track, suggestive of changes at the compact object and accretion disc, but did not reveal the nature of the changes. It was found that quasi-periodic oscillations (QPO) exhibit systematic changes around the Z-track (e.g. van der Klis et al. 1987; Hasinger & van der Klis 1989). Clearly, investigation of the spectral evolution along the Z-track is likely to reveal the nature of the changes; however, spectral studies of the Z-track sources have been hindered by a lack of agreement over which emission model for LMXBs to use.

1.1. Spectral fitting

The nature of X-ray emission in LMXBs has been controversial with two main types of model for the continuum: the first is the Eastern model comprising multi-colour blackbody emission from the inner accretion disc plus non-thermal emission from a central Comptonizing region (Mitsuda et al. 1989); the second model discussed below comprises neutron star blackbody emission plus Comptonization in an extended corona. Previous spectral fitting of the Z-track sources has been largely based on the Eastern model. Spectral evolution along the Z-track in several sources was investigated by Schulz & Wijers (1993) and Schulz et al. (1989). More recently, spectral fitting of the source Cyg X-2 was carried out by Done et al. (2002) using the Eastern model. Spectral fitting results were given in terms of the parameters of the disc blackbody and thermal Comptonization emission components, but it was not clear what caused the parameters to change in the way found. The same model was used by Agrawal & Sreekumar (2003) to fit *Rossi-XTE* spectra of GX 349+2. Spectral fitting of broadband *BeppoSAX* data was carried out

Article published by EDP Sciences and available at http://www.aanda.org or http://dx.doi.org/10.1051/0004-6361:20065035

for GX 17+2, GX 349+2 and for Cyg X-2 (di Salvo et al. 2000, 2001, 2002) who argued that all three sources could be fitted by the Eastern model. In GX 17+2 and GX 349+2, there was little change in blackbody parameters with position on the Z-track, however, in Cyg X-2 there was an increase of blackbody temperature and decrease of blackbody radius moving from the horizontal to the normal branch, suggesting that the inner disc radius was shrinking although an explanation of this was not proposed.

Theoretical models for the Z-track sources have been proposed (Psaltis et al. 1995), involving a magnetosphere at the inner accretion disc, and changes in the geometry and extent of the magnetosphere. However, it has not been possible to test this model in detail, as, for example, the geometry cannot be determined. This modelling also assumes the main element of the Eastern model, that the Comptonizing region is a small central region, and evidence (below) does not support this.

1.2. Approach of the present work

Thus previous spectral fitting based on the Eastern model has not produced a clear explanation of the Z-track and there is now substantial evidence against this model provided by the dipping class of LMXBs. In these sources with high inclination (65−85°), absorption of the X-ray emission takes place on every orbital cycle in the bulge in the outer disc. Complex spectral evolution in dipping strongly constrains emission models providing substantial evidence for a model comprising simple, unmodified blackbody emission from the neutron star and Comptonized emission from an extended accretion disc corona of radial extent R typically 50 000 km, and height H having $H/R < 1$ (the "Birmingham model"; Church & Bałucińska-Church 1995, 2004). The extended size of the ADC is demonstrated by dip ingress timing (Church & Bałucińska-Church 2004) which allows measurement of the ADC radial extent. The spectra of the dipping LMXBs in the non-dip state and in every stage of dipping from many observations have been well-fitted using this model (Church et al. 1997, 1998a,b, 2005; Bałucińska-Church et al. 1999, 2000; Smale et al. 2001; Barnard et al. 2001), and so the evidence for the model is substantial and hence argues against the Eastern model with a small central Comptonizing region.

It should not be thought that the spectral model used is ad hoc, i.e. having a simple form easily implemented that happens to fit the spectra, but with possibly large inaccuracies. The form used is BB + CPL, where BB is simple blackbody emission from the neutron star and CPL is a cut-off power law representing Comptonization. The correct form for Comptonization is very dependent on the correct specification of the seed photon spectrum. With an extended ADC, the seed photons must originate in the disc below the corona with a large population of soft photons below 0.1 keV from large radii. We previously showed that a power law or cut-off power law represents Comptonization well allowing for this, and the Comptonized spectrum continues to rise below 1 keV (Church & Bałucińska-Church 2004) whereas the COMPTT model often used incorporates a blackbody seed photon spectrum decreasing strongly below 1 keV. We have never been able to detect any departure of the thermal emission from simple blackbody form, and we previously reviewed the evidence for use of a simple blackbody and discussed in detail how possible modification in the neutron star atmosphere depends critically on the electron density which is very poorly known (Bałucińska-Church et al. 2001). Kuulkers et al. (2002) also present evidence that X-ray burst emission is of simple blackbody shape.

Finally, when the spectra of LMXBs are fitted with the Eastern model in the form disc blackbody + cut-off power law (e.g. Church & Bałucińska-Church 2001), it is often found that the inner radius of the disc blackbody is unphysically small with values less than 1 km, i.e. substantially less than the neutron star radius. Done et al. (2002) argued that this was purely an artefact of using an incorrect form (cut-off power law) for the Comptonized emission. The above argument shows that, on the contrary, the cut-off power law is a proper description of the Comptonized spectrum if the ADC is extended (at least below the high energy cut-off) as discussed fully in Church & Bałucińska-Church (2004). Thus the conclusion that the Eastern model gives unphysically small inner disc radii is valid, and in addition, modelling based on assuming seed photons that are blackbody with $kT \sim 1$ keV as in COMPTT is invalid.

Thus the approach used in the present work consists of applying for the first time the Birmingham emission model to the Z-track sources, as it provided a good explanation of the dipping LMXBs, to determine whether this model suggests an explanation of the Z-track phenomenon. We chose the source GX 340+0 since high quality *Rossi-XTE* data extending round the full Z-track were available. The source was classified as a Z-track source by Hasinger & van der Klis (1989). QPO were found in *Exosat* data (van Paradijs et al. 1988) and in *Ginga* data (Penninx et al. 1991) and kilohertz QPO were discovered by Jonker et al. (1998). The detection of radio by Penninx et al. (1993) is important indicating the presence of jets. Fender & Hendry (2000) summarized previous work on radio detection from X-ray binaries showing that radio emission is detected from black hole binaries and from the Z-track sources when on the horizontal branch, concluding that a requirement for jet formation was an X-ray luminosity approaching the Eddington limit, i.e. greater than 0.1 $L_{\rm Edd}$. More recently, Migliari & Fender (2006) summarize the detection of relatively weak radio emission from a number of Atoll sources.

1.3. A monotonic increase of mass accretion rate?

Finally, we address a widely-held view that the observed hardness changes in the Z-track sources are driven in some way by a mass accretion rate $\dot{M}$ which increases monotonically around the Z-track in the direction HB-NB-FB. The movement round the track on timescales of hours, without jumping between tracks, suggested the variation of a single parameter, probably $\dot{M}$ (Priedhorsky et al. 1986). In a multi-wavelength campaign (Hasinger et al. 1990), Cyg X-2 was observed in X-ray, ultraviolet, optical and radio. The results of the *IUE* observations (Vrtilek et al. 1990) showed an increase of intensity for motion HB-NB-FB. However, the identification of these data with the flaring branch depended on strong variability which was probably due to X-ray dipping, and omitting these data would mean that there is no very dramatic correlation of UV with track position. Van Paradijs et al. (1990) presented evidence for increase of optical emission line strength for motion HB-FB but noted that the number of data points was rather limited, while absorption line strength decreased, indicating that the processes involved are complex and can involve X-ray reprocessing.

A monotonic increase of $\dot{M}$ around the Z-track in the direction HB-NB-FB is, of course, inconsistent with the basic observational fact that the X-ray intensity *decreases* between the hard apex and soft apex. A monotonic increase of $\dot{M}$ is not an assumption of the Eastern model; however Agrawal et al. (2003) suggested that the results of fitting this model might be qualitatively consistent with a monotonic increase. It would be

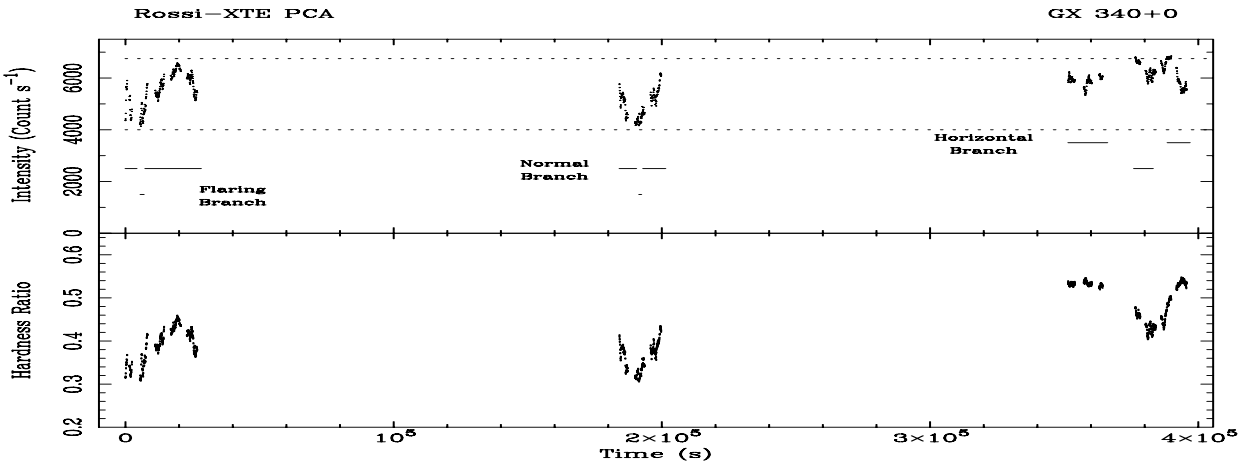

Fig. 1. *Top*: background-subtracted and deadtime-corrected PCA light curve of the 1997 September observation of GX 340+0 with 64 s binning. Parts of the lightcurve are identified (see text) with branches of the Z-track (Fig. 2) and shown as horizontal bars. Most of the first half of the observation is on the Normal Branch except for two large flares as shown; the second half of the observation is mostly on the Horizontal Branch. The dotted lines emphasize the upper and lower intensity limits which are consistent across the observation: these limits correspond to the intensities of the Hard Apex and Soft Apex of the Z-track. *Bottom*: the corresponding variation of hardness ratio (7.3−18.1 keV)/(4.1−7.3 keV).

necessary for the Comptonized emission luminosity to decrease from hard to soft apex while $\dot{M}$ increased. In the present work, the luminosity decrease by a factor of two seems unlikely if $\dot{M}$ were increasing.

Kuulkers et al. (2002) provided another argument against the increase of $\dot{M}$ around the Z-track. Unstable nuclear burning is expected at various mass accretion rates (Fujimoto et al. 1981; Fushiki & Lamb 1987; Bildsten 1998; Schatz et al. 1999) including accretion rates close to the Eddington $\dot{M}$ due to He burning in a mixed H/He environment, i.e. $1.0 \times 10^{-9} < \dot{M} < 2.6 \times 10^{-8}\ M_{\odot}\,\mathrm{yr}^{-1}$ (Bildsten 1998). At higher mass accretion rates corresponding to luminosities greater than 3×10^{38} erg s^{-1}, burning is expected to be stable. Thus, Kuulkers et al. argued that unstable nuclear burning should be observed in the Z-track sources, and X-ray bursting is not, in general, seen. Bursts are seen in GX 17+2 and Cyg X-2 (Kahn & Grindlay 1984; Tawara et al. 1984; Sztajno et al. 1986; Kuulkers et al. 1995; Wijnands et al. 1997; Smale 1998). However, bursting in these sources showed no correlation of burst properties with Z-track position (Kuulkers et al. 1995, 1997) as expected if the mass accretion rate was changing substantially along the Z-track. It thus appears that the increase of $\dot{M}$ around the Z-track cannot be regarded as proven, and the results presented here will be viewed in this context.

2. Observations and analysis

Several observations have been made of GX 340+0 with the *Rossi X-ray Timing Explorer* satellite. We examined the data in the HEASARC archive remotely obtaining hardness-intensity plots for all observations of this source, and selected data covering a full Z-track in a relatively short time (to prevent assembling data in which several Z-tracks occurred, shifted with respect to each other, which would confuse the analysis). We analysed the long observation made in 1997 September, consisting of four sub-observations each of between 5 and 8 h duration and spanning a total time of 400 ks, starting on September 21 and ending on September 25. Data from both the proportional counter array (PCA) and the high-energy X-ray timing experiment (HEXTE) were used (full bands: 2−60 keV and 15−250 keV, respectively). The PCA was in Standard2 mode with 16 s resolution. It consists of five Xe proportional counter units (PCU) with a combined effective area of about 6500 cm^2 (Jahoda et al. 1996). Examination of the housekeeping data showed that all 5 PCUs were reliably on during this observation. Light curves and spectra were extracted using the standard *RXTE* analysis software FTOOLS 5.3.1. PCA lightcurves were extracted from the raw data for the top layer of the detector as normal using both left and right anodes. Standard screening was applied to select data with an offset between the source and telescope pointing direction of less than 0.02°, and elevation above the Earth's limb of more than 10°. A lightcurve was extracted in the energy band 1.9−18.5 keV. The program PCABACKEST was used to generate background files corresponding to each PCA raw data file and these were used for background subtraction. The latest background model was applied, specifically the "bright" model recommended for Epoch 3 of the mission (defined as 1996 April 15−1999 March 22). Deadtime correction was carried out using dedicated software encapsulating the prescription provided by the mission specialists. The background-subtracted, deadtime-corrected lightcurve is shown with 64 s binning in Fig. 1 (top panel). PCA lightcurves were also extracted in three bands spanning the total band used in Fig. 1: 1.9−4.1 keV (low band), 4.1−7.3 keV (medium band) and 7.3−18.5 keV (high band). From these, a hardness-intensity plot was constructed defining hardness as the ratio of high/medium. This full Z-track is shown in Fig. 2.

Lightcurves and spectra were also extracted from Cluster 1 of the HEXTE instrument, so that simultaneous spectral fitting of PCA and HEXTE data could be carried out. These were extracted with the FTOOL HXTLCURV which also provided background files and allowed deadtime correction based on the deadtime coefficients file of 2000 February.

3. Results

3.1. The X-ray lightcurve and the Z-track

Figure 1 shows the strong variability of GX 340+0 during these observations. Firstly, an identification was made of each part of the PCA lightcurve with position on the Z-track (Fig. 2). Individual short segments of data were selected from the lightcurve using the FTOOL MAKETIME and for each segment a hardness-intensity plot made so as to reveal the Z-track

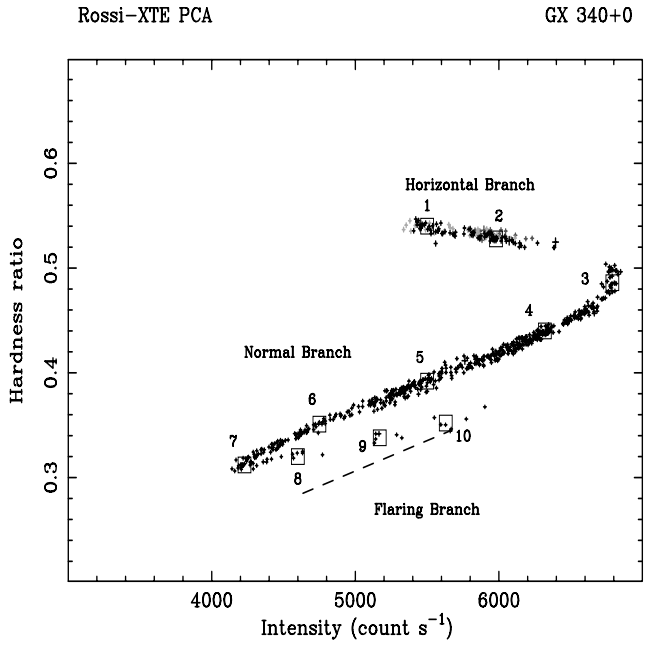

Fig. 2. Z-track of the observation derived from background-subtracted and deadtime-corrected lightcurves with 64 s binning. Intensity is in the band 1.9−18.1 keV and hardness ratio is (7.3−18.1 keV)/(4.1−7.3 keV). The boxes show the ranges of intensity and hardness ratio used for selection of PCA and HEXTE spectra, and are labelled 1−10 starting from the Horizontal Branch end of the Z-track. The dashed line shows the position of 7 data points removed before analysis (see text).

position of each, and these identifications are labelled in Fig. 1. The lower panel shows the hardness ratio (HR) as a function of time from which the positive correlation of HR and intensity on the normal branch can be seen, as well as the reciprocal variation on the HB. The source spent most time in the horizontal and normal branches, and it can be seen that the source intensity varied between two levels shown as dotted lines. At the start of the observation the source moved along the normal branch from the soft apex to the hard apex, the intensity increasing from 4000 to 6800 count s^{-1} per PCU. In the central sub-observation, the source moved down the normal branch to lower intensities and then back to higher intensities on this branch. In the third and fourth sub-observation, the source was mostly on the horizontal branch; i.e. having an intensity reduced from the upper limit found at the hard apex. Two short sections of data were on the flaring branch, each about 1000 s in duration, i.e. there were two flares; however, the intensity of the source was so high that these provided more than adequate counts for high quality spectral fitting (below). A section of data near the start of the observations did not lie on any of the three normal branches, but extended downwards from the extreme end of the flaring branch. Such behaviour has previously been seen, for example in GX 5-1 by Kuulkers et al. (1994), and is thought to relate to X-ray dipping. As the aim of the present work is to understand the normal Z-track, a selection was made to remove about 800 s of data showing this behaviour.

3.2. Spectral analysis

The Z-track shown in Fig. 2 is derived from lightcurves with 64 s binning. Increasing the bin size from the intrinsic 16 s binning of PCA Standard 2 data reduces the width of the Z-track at all points. More important, our previous work (e.g. Barnard et al. 2003) has shown that data should be selected on a line through the centre of the Z-track as we are interested in the changes taking place along the track and not perpendicular to it. We select spectral data at positions about equally spaced along the Z-track by defining boxes in the hardness-intensity plane and selecting data within each box. A good time interval (GTI) filter was produced for each selection consisting of the time intervals when data were inside each box and used for extraction of lightcurves and spectra. A hardness-intensity plot was then made for the selected data and overlayed on the full Z-track to see how good the selection was, checking that points lie on a smooth curve not deviating appreciably perpendicular to the Z-track.

A total of 10 spectra were extracted with three spectra on the HB (one at the hard apex), four on the NB including one at the soft apex, plus three on the FB. The ranges of intensity were generally 100 count s^{-1} wide, e.g. from 6050−6150 count s^{-1} with a range of hardness ratio in this case from 0.425−0.435. For each selection, PCA spectra were extracted and the corresponding background spectra generated. Deadtime correction was made to source + background (S + B) spectra and to background (B) spectra using a local facility PCADEAD. Pulse pileup correction was found to have negligible effect and so was not made. A systematic error of 1% was applied to each channel as is standard practice in analysing PCA data; it was not necessary to regroup data to a minimum count per bin for use of the χ^2 statistic as the count in raw channels was already high (e.g. typically 200).

HEXTE spectra were also extracted from Cluster 1 for detectors 0, 1 and 3, detector number 2 having failed in March 1996. Data were selected using the GTI filter files generated from PCA data using the *RXTE* FTOOL HXTLCURV which also deadtime corrected the output files. This produced a source + background and a background spectrum from each raw data file, which were then added to form a single S + B spectrum and a single B spectrum. The auxiliary instrument response file (arf) of May 2000 was used, together with the response matrix file (rmf) of March 1997. The rmf file was rebinned to match the actual numbers of channels in the HEXTE spectra using the FTOOLS RDDESCR and RBNRMF. The energy ranges used in the fitting were set by examining the energies at which the spectral flux density of the background became equal to that of the source + background. Typically, the ranges used were 3.5−30 keV in the PCA and 18−40 keV in HEXTE.

The aim of this work was to determine whether application of a particular emission model (the Birmingham model) would provide a good fit to spectra and suggest the nature of the changes taking place, and so an explanation of the Z-track. Thus it was not the intention to fit a variety of two-component models as it is widely appreciated that various models can give acceptable fits, and it is not sensible to try to choose between physical models on the basis of rather small differences in χ^2. In particular, as discussed in Sect. 1, the evidence against the Eastern model is now strong and so in the present work the Birmingham model was applied but with extensive testing of various aspects of the fitting.

Firstly, it was clear from examining the residuals when a continuum only model was applied that a broad iron line was present, and the width of the peak in the residuals suggested a half-width of the line σ of ~0.5 keV. Fitting with and without a line made the significance of the line clear: without a line, spectrum 2 gave a χ^2/d.o.f. of 66/61 improving to 46/60 for a line at energy 6.5 keV. In the final fitting, the line energy was free and a systematic variation around the Z-track was seen (Sect. 3.2.3), and for spectrum 2, freeing the energy further improved χ^2/d.o.f.

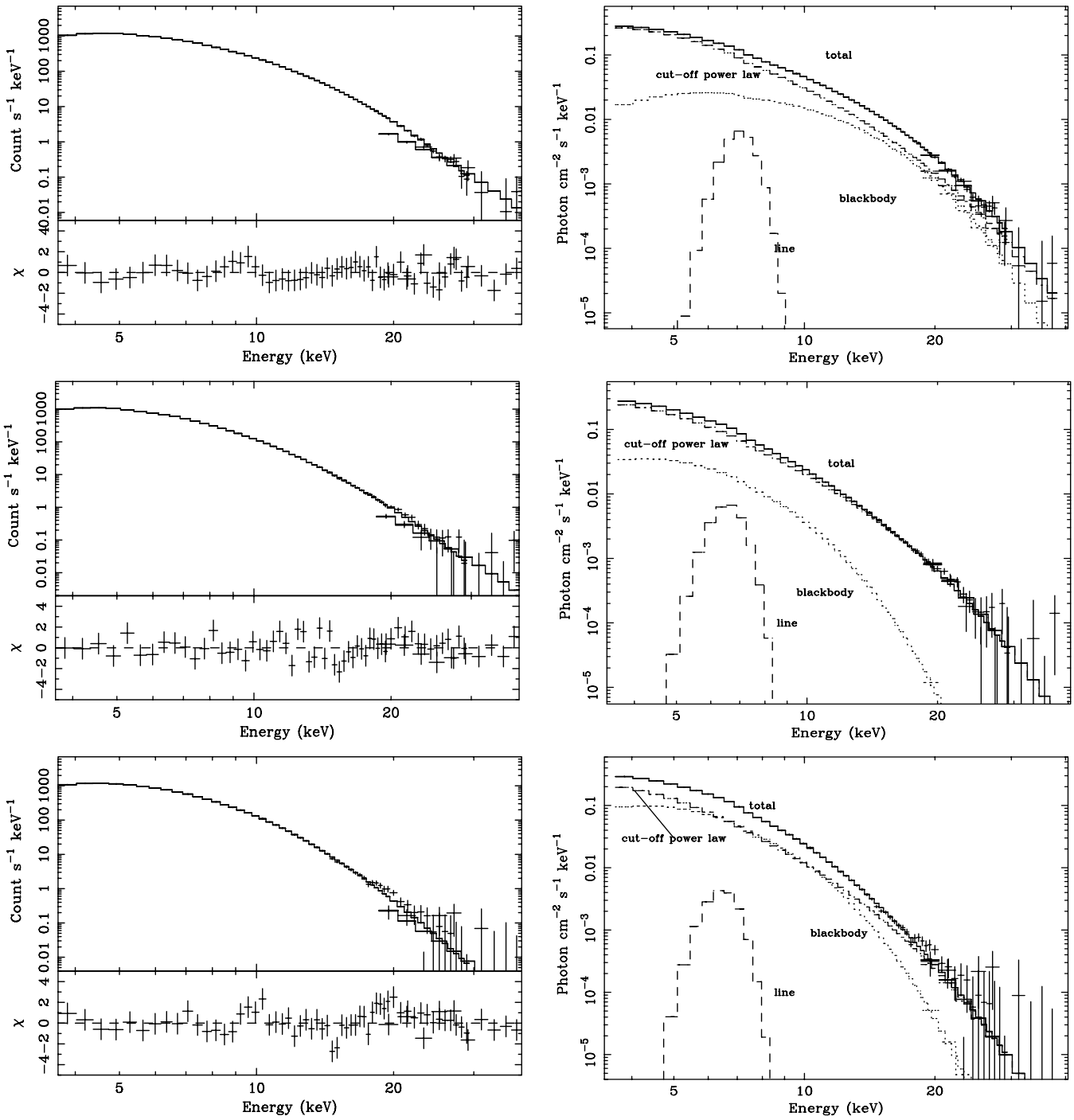

Fig. 3. Spectra for the HB (*top*; spectrum 2), NB (*centre*; spectrum 6) and FB (*bottom*; spectrum 9). Both the PCA and HEXTE data are shown, in each case with the folded data (*left*) with residuals and unfolded data (*right*). Over large parts of each spectrum the error bars are too small to be visible. Model components are labelled in the unfolded spectra.

to 41/59. With the inclusion of a Gaussian line in the spectral model, good values of χ^2/d.o.f were obtained at all positions on the Z-track for the model BB + CPL + GAU; i.e. a simple blackbody from the neutron star, Comptonized emission specified by a cut-off power law as discussed in Sect. 1, plus the Gaussian line (the emission site of the line is discussed in Sect. 3.2.3). For the blackbody component, the fitting providing well-determined values for the blackbody temperature $kT_{\rm BB}$ and normalization. From the normalization, defined as the luminosity adjusted to a source distance of 10 kpc, the blackbody radius $R_{\rm BB}$ was derived via $L_{\rm BB} = 4\pi R_{\rm BB}^2 \sigma T_{\rm BB}^4$ where $L_{\rm BB}$ is the luminosity of the blackbody component and σ is Stefan's constant. A clear pattern of behaviour of $kT_{\rm BB}$ and $R_{\rm BB}$ along the Z-track emerged, and there was also a clear pattern of behaviour of the luminosities $L_{\rm BB}$ and $L_{\rm CPL}$. Thus the spectral fitting results were robust.

With high luminosity sources such as GX 340+0, the Comptonized emission does not extend to very high energies as the cut-off energy $E_{\rm CO}$ is relatively low, i.e. a few keV (e.g. present work; Barnard et al. 2003) when compared with typical X-ray burst sources such as XB 1916-053 with much smaller luminosities. In the case of such sources, broadband spectra especially from the *BeppoSAX* satellite extending from 0.1−100 keV

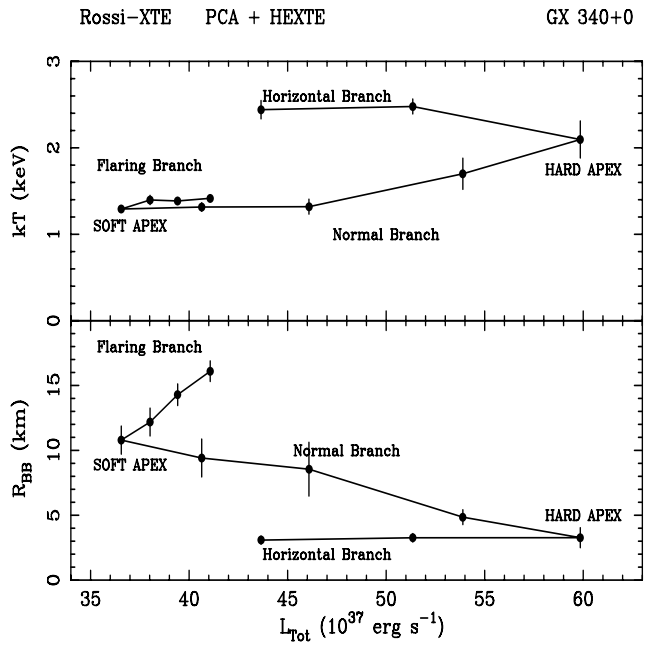

Fig. 4. Variation of neutron star blackbody temperature and radius along the Z-track showing the monotonic changes of each on both the Normal and Horizontal Branch, i.e. with no sudden change at the Hard Apex, unlike the non-thermal emission (see Fig. 6).

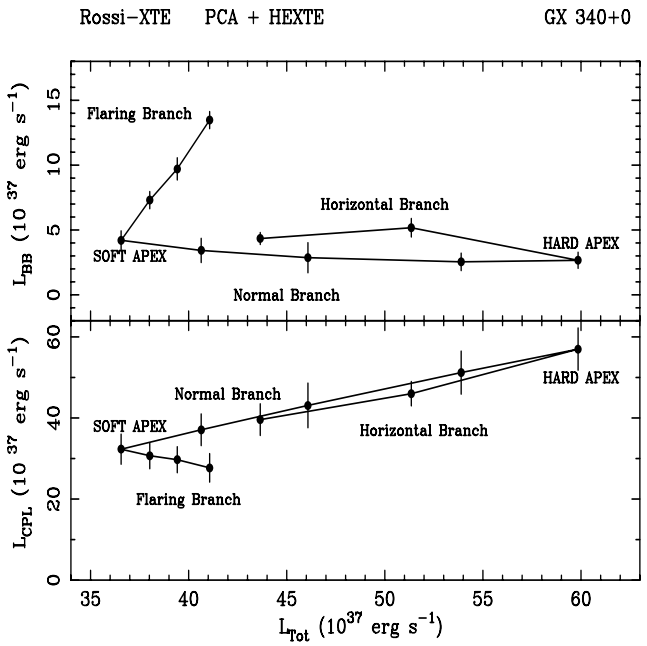

Fig. 5. Variation of the luminosities of the two continuum components along the Z-track showing the marked increase of the Comptonized emission on the Normal Branch and a similar decrease on the Horizontal Branch.

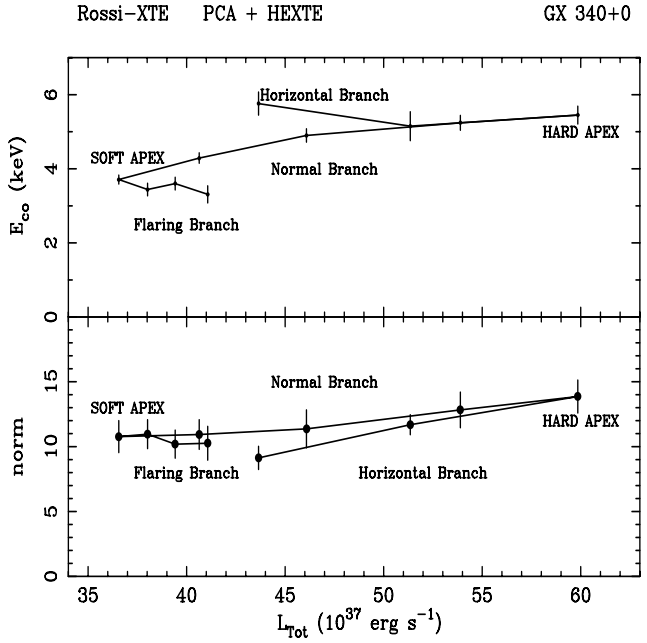

Fig. 6. Variation of the normalization and cut-off energy of the Comptonized emission along the Z-track.

or more can be used to provide E_{CO} and the value of the power law photon index Γ. In XB 1916-053, E_{CO} was found to be 80 ± 10 keV (Church et al. 1998b). In the present data it was found that E_{CO} was well-determined in the spectral fitting, varying between 3 and 6 keV depending on position in the Z-track. However, the low value of cut-off energy restricts the range of energy available for determination of the power law index and the procedure was adopted of fixing Γ at 1.7. This value is physically reasonable as it corresponds to a low Comptonizing region temperature and high optical depth (Shapiro et al. 1976). After fitting to obtain all other parameters, the index was freed, and it was found that it remained close to 1.7. Extensive testing revealed that the pattern of behaviour shown in Figs. 4−6 was always the same and did not depend on the value of the power law index. Similarly, we adopted the procedure previously used (e.g. Barnard et al. 2003) when an emission line is broad and fixed the Gaussian half-width σ at 0.5 keV to prevent the line absorbing neighbouring continuum. Good fits were obtained to all spectra; χ^2/d.o.f. appears marginally high for spectrum 7, but it is difficult to be sure of the precise level of systematic error to use for a bright source in which Poisson errors are negligible. The systematic error added in general to data from a given observatory is based on calibrations and an instrument response that is improved during the mission. However, calibrations are not carried out using the brightest sources, and so the 1% used here may be too low, as we previously found in the case of Sco X-1 (Barnard et al. 2003), and if systematic errors of 1.5% are used, χ^2/d.o.f. becomes 57/60 for this spectrum.

The low energy limit of the PCA instrument (normally set in spectral fitting at ∼3 keV) mitigates against determination of the column density N_H, especially if the Galactic column density is low. It is often the case in fitting *RXTE* spectra that the value of N_H has to be fixed at the known Galactic value. In the present data, acceptable fits were only obtained with values of $N_H \sim 8 \times 10^{22}$ atom cm^{-2}, several times higher than the Galactic value of $\sim 2.2 \times 10^{22}$ atom cm^{-2} (Dickey & Lockman 1990), suggesting absorption intrinsic to the source. (When we fitted the Eastern model to a number of spectra, an even higher column density of $\sim 12 \times 10^{22}$ atom cm^{-2} was needed.) With the Birmingham model, fitting with N_H fixed at 8×10^{22} atom cm^{-2} produced acceptable fits for all spectra. However, careful investigation revealed a systematic change of N_H along the Z-track, with the column density increasing along the normal branch towards the hard apex and then decreasing on the horizontal branch. Thus N_H was allowed to be free except for the spectra on the flaring branch (spectra 7−10) where somewhat reduced count statistics limited the ability to determine N_H. The effect

Table 1. Spectral fitting results: column density, blackbody temperature $kT_{\rm BB}$, normalization and blackbody radius $R_{\rm BB}$; power law cut-off energy $E_{\rm CO}$ and normalization; line energy $E_{\rm l}$ and equivalent width; goodness of fit. 90% confidence errors are shown.

spectrum	$N_{\rm H}$	kT keV	$norm_{\rm BB}$	$R_{\rm BB}$ km	$E_{\rm CO}$ keV	$norm_{\rm CPL}$	$E_{\rm l}$ keV	EW eV	χ^2/d.o.f.
Horizontal Branch									
1	9.2 ± 0.8	2.44 ± 0.11	3.6 ± 0.4	3.1 ± 0.3	5.8 ± 0.3	9.13 ± 0.9	6.9 ± 0.4	81	27/59
2	10.2 ± 0.8	2.48 ± 0.09	4.3 ± 0.6	3.3 ± 0.3	5.2 ± 0.4	11.7 ± 0.8	7.1 ± 0.4	75	41/59
3	10.6 ± 0.8	2.10 ± 0.21	2.2 ± 0.5	3.3 ± 0.8	5.4 ± 0.2	13.9 ± 1.3	7.1 ± 0.4	68	39/59
Normal Branch									
4	9.5 ± 0.8	1.70 ± 0.18	2.1 ± 0.6	4.9 ± 0.6	5.2 ± 0.2	12.8 ± 1.4	6.7 ± 0.4	79	29/59
5	8.8 ± 0.9	1.32 ± 0.09	2.46 ± 1.0	8.6 ± 1.8	4.9 ± 0.2	11.4 ± 1.5	6.6 ± 0.3	80	27/59
6	8.4 ± 0.5	1.32 ± 0.05	2.8 ± 0.8	9.4 ± 1.5	4.3 ± 0.1	10.9 ± 1.1	6.6 ± 0.1	84	63/59
7	8.0	1.29 ± 0.03	3.5 ± 0.6	10.8 ± 1.1	3.7 ± 0.1	10.8 ± 1.2	6.5 ± 0.1	91	92/60
Flaring Branch									
8	8.0	1.40 ± 0.05	6.0 ± 0.6	12.2 ± 1.1	3.4 ± 0.2	11.0 ± 1.1	6.4 ± 0.3	64	65/60
9	8.0	1.39 ± 0.04	8.0 ± 0.7	14.3 ± 0.8	3.6 ± 0.2	10.2 ± 1.1	6.5 ± 0.4	45	70/60
10	8.0	1.42 ± 0.03	11.1 ± 0.5	16.1 ± 0.8	3.3 ± 0.2	10.3 ± 1.3	6.4 ± 0.8	14	63/60

Column densities are in units of 10^{22} atom cm^{-2}; the normalization of the blackbody is in units of 10^{37} erg s^{-1} for a distance of 10 kpc, the normalization of the cut-off power law is in units of photon cm^{-2} s^{-1} keV^{-1} at 1 keV and the line normalization has units of photon cm^{-2} s^{-1}.

in these spectra of fixing $N_{\rm H}$ on the other parameters was small, varying from 1% in one spectrum to less than 15% in another. The final fitting results are shown in Table 1. It can be seen from the 90% confidence limits for $N_{\rm H}$ that the change in column density around the Z-track is significant.

3.2.1. The neutron star blackbody

Results for the blackbody parameters $kT_{\rm BB}$ and $R_{\rm BB}$ as a function of position on the Z-track are shown in Fig. 4. It can be seen from the small size of the 90% confidence error bars that these parameters are well constrained, as is their evolution around the Z-track. The luminosities of the two continuum components are given in Fig. 5, in all cases as a function of the total luminosity $L_{\rm Tot}$ in the band 1−30 keV from the unabsorbed flux of the best-fitting spectral model for each spectrum. A source distance of 10 kpc was assumed based on the considerations of Christian & Swank (1997) who point out that as a bright Galactic source with coordinates ($339\overset{\circ}{.}6-0\overset{\circ}{.}1$) it is likely to be at ∼10 kpc and who found an upper limit of 11 kpc for the distance. The distance is unlikely to be less than 5 kpc as this would be inconsistent with the high column density of the source even allowing for a large amount of intrinsic absorption, and because an optical counterpart would have been detectable. Thus for a distance uncertainty of −50% +10%, absolute luminosities will be known to better than a factor of two, while the pattern of the parameter variations is Figs. 4−6 will not be affected at all by systematic uncertainty in luminosity. From Fig. 4, it can be seen that the blackbody parameters have a systematic evolution along the Z-track. Firstly, the blackbody temperature is smallest at the soft apex at ∼1.25 keV. From this point, the temperature increases as we proceed towards the hard apex, and continues to increase on the horizontal branch. The most striking result is the value of the blackbody radius $R_{\rm BB}$ which is ∼11 km at the soft apex (10.8 ± 1.1 km). In addition to the 10% error from spectral fitting there will be a possible systematic error due to the uncertainty in source distance. $R_{\rm BB}$ decreases continually along the normal branch and the horizontal branch. On the flaring branch, there is a small but significant increase of temperature, but a marked increase of blackbody radius to 16 km. Moreover, in the non-flaring source, $R_{\rm BB}$ is a maximum at the soft apex. The most obvious explanation is that this is the natural limit when the whole surface of the neutron star is emitting, while away from this point, the whole neutron star is not emitting.

On the basis of these results we propose that the soft apex is a quiescent state of the source with the neutron star emitting with its lowest temperature and from the whole of its surface. We next discuss the changes taking place on moving away from the quiescent state of the source and for this, we need to consider the luminosities of the continuum components. Figure 5 shows the evolution along the Z-track of the luminosities of the individual blackbody and Comptonized continuum components as a function of $L_{\rm Tot}$. The major component is the Comptonized emission which varies between $30-55 \times 10^{37}$ erg s^{-1} on the normal branch while $L_{\rm BB}$ is substantially less.

Firstly, consider motion away from the quiescent state towards the hard apex. The most striking result is the strong increase in the luminosity of the Comptonized emission $L_{\rm CPL}$, followed by a decrease on the horizontal branch by about the same amount essentially back along the same path. Application of the spectral model used in the present work has revealed this for the first time. The Comptonized emission arises in the ADC located above the accretion disc and it is expected that the ADC emission will be related to the properties, particularly the density of the accretion disc, depending on the mass accretion rate $\dot{M}$. We suggest that it is *highly unlikely* that this strong increase of luminosity of the Comptonized emission could take place without an increase of $\dot{M}$, and so propose that the evolution of $L_{\rm CPL}$ is caused by an increase of $\dot{M}$ on the normal branch. The results (Fig. 5) imply that it is followed by a decrease of $\dot{M}$ back to about the initial value on the horizontal branch. We point out here that under the conditions of high radiation pressure that exist at the hard apex and HB (below), the measured value of $L_{\rm Tot}$ may not give the true $\dot{M}$ as appreciable mass accretion can be diverted into the jets such that the mass accretion rate may not actually decrease when the source gets to the hard apex, but that this may happen at some later time. This is discussed in Sect. 4.2.

This does not support the previously held view that $\dot{M}$ changes monotonically along the Z-track (increasing in the direction HB – NB – FB), since we propose that the mass accretion rate increases from the soft apex to the hard apex. If this is so, then it suggests that the evidence from previous work of an increase in UV or optical emission around the Z-track (Sect. 1.3) is not conclusive, or if an increase were confirmed, that this does not imply an increase of mass accretion rate. The blackbody

luminosity behaves quite differently from that of the Comptonized emission not reversing its trend at the hard apex but continuing to increase on the horizontal branch reflecting the smooth variation of $kT_{\rm BB}$ which increases on both the normal and horizontal branches, and of $R_{\rm BB}$ which decreases on both branches (Fig. 4). This suggests that the same process is affecting the blackbody emission on the two branches.

Figure 4 shows that the blackbody temperature $kT_{\rm BB}$ increases from ∼1.3 keV in the quiescent state of the source at the soft apex to 2.0 keV at the hard apex, and 2.4 keV on the horizontal branch, and we propose that this increase is due to an increasing mass accretion rate. Most of the change takes place between the upper half of the normal branch and halfway along the horizontal branch. Beyond this point the temperature appears to have reached a stable value. Similarly, the blackbody radius decreases from ∼11 km at the soft apex to ∼3 km on the horizontal branch. The change in $kT_{\rm BB}$ by about a factor of two will mean that the radiation pressure of the neutron star emission varying as T^4 will increase by nearly a factor of 10. At the same time the emitting area shrinks from the whole neutron star down to a narrow equatorial belt. The half-height h of this belt is calculated from $R_{\rm BB}$ since the area $A = 4\pi R_{\rm BB}^2 = 4\pi hR$ (the surface area of a sphere intersected by two parallel planes $2h$ apart, where R is the radius of the neutron star assumed to be 10 km). On the horizontal branch, h is close to 1.0 km. The inner disc in bright sources is radiatively-supported, i.e. not thin, but extends vertically tens of kilometres above the orbital plane (Frank et al. 2002). We propose that the strong radiation pressure of the neutron star removes the outer layers of the inner disc (acting close to vertically upwards) while having little effect on the disc in the orbital plane where it acts horizontally into the disc. In Sect. 4.1 we show that the decrease in blackbody area is consistent with disruption of the inner disc. In addition, the observed increase of column density provides direct evidence for disruption of the inner disc, or at least for release of material somewhere within the source. Detailed modelling is desirable to demonstrate the disruption of the inner disc proposed.

Moreover, we can see the strength of the increased radiation pressure by comparison with the Eddington limit. For the source at the horizontal branch end of the Z-track, $L_{\rm BB}$ is 4.3×10^{37} erg s^{-1}, i.e. 0.25 $L_{\rm Edd}$ while the total luminosity is 4.4×10^{38} erg s^{-1}. Using the blackbody radius of 3.08 km we find that the flux emitted by the surface f is 3.6×10^{25} erg cm^{-2} s^{-1}. On the surface of the star at $r = R$, the critical Eddington flux $f_{\rm Edd}$ is $L_{\rm Edd}/4\pi R^2$, i.e. 1.4×10^{25} erg cm^{-2} s^{-1} (for a neutron star radius of 10 km). Thus at this position on the Z-track, the flux is super-Eddington and when we are close to the narrow equatorial strip we may expect strong effects due to the high radiation pressure. By contrast, at the soft apex, the blackbody luminosity is similar at 4.2×10^{37} erg s^{-1} to that at the end of the Z-track, but the flux emitted is fifteen times reduced at 0.24×10^{25} erg cm^{-2} s^{-1}, substantially sub-Eddington. The variation of $f/f_{\rm Edd}$ along the Z-track is given in Fig. 7 showing that the ratio increases to more than unity on the normal branch reaching a maximum on the horizontal branch.

Moving from the soft apex onto the flaring branch, the most obvious feature is the approximate constancy of the Comptonized emission luminosity. This is strongly suggestive that the mass accretion rate does not change on this branch, since any significant change would surely result in $L_{\rm CPL}$ changing. However, there are strong changes in the neutron star blackbody with the luminosity increasing by a factor of three. While $kT_{\rm BB}$ displays only a small increase of less than 10%, there is a large increase in emitting area (blackbody radius).

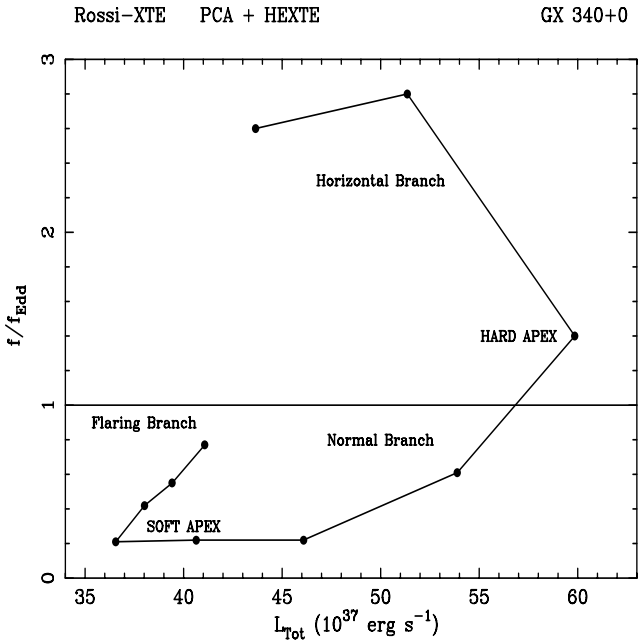

Fig. 7. The neutron star emitted power per unit area relative to the Eddington flux showing that the effects of radiation pressure are strong on the upper normal and horizontal branches.

The nature of flaring in such sources has been controversial. The view of a monotonically increasing $\dot{M}$ around the Z-track implies that an increase of mass accretion rate causes flaring. Alternatively, the flares may be thermonuclear and the present results with implied constant $\dot{M}$ suggest this quite strongly. Thus lower luminosity LMXBs often exhibit unstable burning as X-ray bursting while brighter sources exhibit flaring. The implied constancy of $\dot{M}$ on the flaring branch again disagrees with the often held view that $\dot{M}$ increases monotonically on the Z-track in the direction HB–NB–FB.

On the flaring branch, the blackbody radius increases to 16 km so that if the whole neutron star is emitting at the soft apex, then the emission may spread beyond the neutron star in flaring, as discussed in Sect. 4.3. The radiation pressure also increases. From the soft apex to the spectrum near the peak of flaring (spectrum 10) $L_{\rm BB}$ increases by a factor of three (due to $R_{\rm BB}$ increasing). Allowing for the area increase, the emitted flux increases by 50% while the Eddington flux $L_{\rm Edd}/4\pi R^2$ decreases to 5.4×10^{24} erg cm^{-2} s^{-1} for spectrum 10, so that $f/f_{\rm Edd}$ increases from 0.24 at the soft apex to 0.77 in spectrum 10, and is presumably close to 1.0 at the actual flare peak, for which there was no spectrum (see Fig. 7).

3.2.2. The Comptonized emission

The variation of the cut-off energy and the normalization of the Comptonized emission are shown in Fig. 6. Both of these were well-determined in the fitting. The normalization, of course, mirrors the behaviour of $L_{\rm CPL}$. The cut-off energy $E_{\rm CO}$ is correlated with the blackbody temperature, suggesting a link between the neutron star emission and the properties of the ADC. This is certainly true on the normal and horizontal branches. The cut-off energy reflects the electron temperature $kT_{\rm e}$ of the ADC plasma, such that for high optical depth to electron scattering $E_{\rm CO} = 3kT_{\rm e}$ (e.g. Petrucci et al. 2001). The observed correlation suggests that the ADC electron temperature is responding to changes in the neutron star temperature.

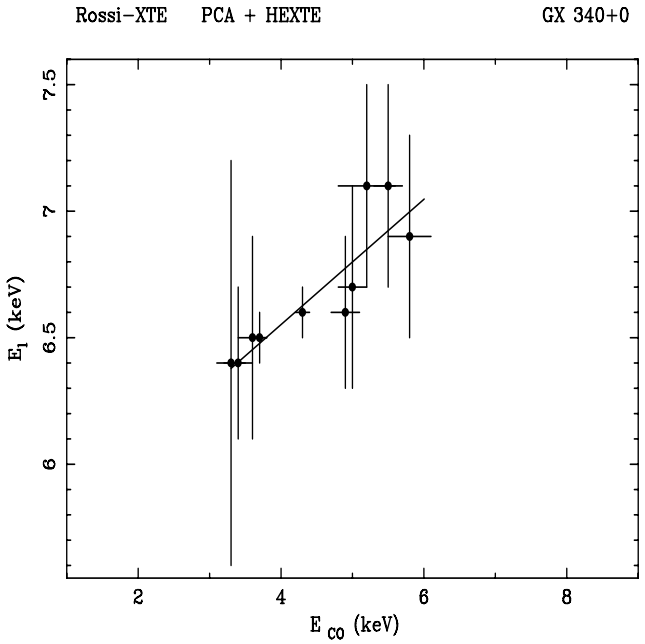

Fig. 8. Correlation of Fe line energy with the cut-off energy of the Comptonized emission.

Our previous work is consistent with a single ADC electron temperature: if the ADC temperature varied substantially as the disc temperature does, say by a factor of ten, we would expect the knee at the Comptonization cut-off to be spread over a factor of ten in energy, e.g. from 2.5 to 25 keV which would be very obvious. We have never detected any departure from a single cut-off energy in any of our work on LMXBs (e.g. Church et al. 1997). Moreover, there is other evidence that the ADC is isothermal. In lower luminosity sources, the cut-off energy is generally high (e.g. di Salvo & Stella 2002) implying a high electron temperature of 25 keV or more, although this is not understood since theoretically kT_e should be limited to the inverse Compton temperature, i.e. less than ~3 keV. Thus there must be a presently unknown process heating the corona. In brighter sources ($L > 10^{37}$ erg s^{-1}), the cut-off energy falls to a few keV, and the neutron star and ADC temperatures are equal (Bałucińska-Church & Church 2005) indicating thermal equilibrium between the neutron star and ADC which could be due to the higher plasma density in the ADC giving high thermal conductivity. This also suggests that there is thermal equilibrium within the ADC resulting in the ADC being isothermal. Thus, the use of a simple cut-off power law within the Birmingham model is justified on the basis of an isothermal ADC.

In the present data on GX 340+0, the average ratio of E_{CO}/kT_{BB} from the spectral fitting results is 2.49 ± 0.46 at 67% confidence. The constancy of the ratio along the Z-track is striking and the closeness of the average to 3.0 implies that the ADC temperature is equal to the blackbody temperature if the plasma has high optical depth.

3.2.3. The line emission

Table 1 shows the dependence of the observed iron line energy on Z-track position with the lowest energy at the soft apex, systematically increasing along the NB to the hard apex, remaining high on the HB. There is a good correlation of the line energy with E_{CO}, as shown in Fig. 8, since a linear fit to these data taking into account the 90% confidence errors in both y and x gives a slope of 0.25 ± 0.04 which is inconsistent with zero slope, and the correlation coefficient is 0.985. The cut-off energy is a measure of the electron temperature in the ADC, and Fig. 8 provides clear evidence for the origin of the line in the ADC, important because the site of line emission in LMXBs has been controversial. The line energy at the soft apex of ~6.5 keV suggests a low ionization state while at the hard apex for the energy of ~7 keV the state is high (Makishima 1986). The ionization state will increase if the ionization parameter $\xi = L/n\,r^2$ increases. At the soft apex the whole neutron star emits isotropically, but at the hard apex, the radiation from an equatorial strip becomes concentrated towards the disc and ADC so increasing ξ substantially, and this would explain the increased line energy at the hard apex.

There is little evidence for the line normalization changing systematically, and so the equivalent width (*EW*) appears approximately constant. However, there is an apparent decrease of *EW* in flaring. The normal calculation of *EW* compares the line flux with the total continuum flux, and the continuum emission of the ADC where the line appears to be generated has constant luminosity in flaring. If the *EW* is calculated on the basis of this ADC continuum component and not the total, there is no decrease in *EW* (in spectra 8 and 9) and only a possible decrease for spectrum 10.

4. Discussion

We have investigated spectral changes along the Z-track based on the use of a particular emission model. In the following we examine the implications of the results on the assumption that this model is correct. As discussed in Sect. 1, we do not know of any major inaccuracy in use of the spectral form BB + CPL within the model, and it is difficult to quantify any small level of inaccuracy. However, such inaccuracy will not change the *pattern* of parameter variation around the Z-track and is not expected to lead to large errors in, for example, the blackbody radius at the soft apex. The results provide a plausible physical picture of the Z-track, of the observation of jet radio emission on the horizontal branch and of the nature of flaring, which is quite different from previous pictures. In the model presented here, the constant luminosity of the ADC emission on the FB implies $\dot{M}$ is constant and so flaring must be thermonuclear. The soft apex is the quiescent state of the source, with $\dot{M}$ increasing along the normal branch causing an increase of the ADC luminosity. The neutron star blackbody temperature then rises causing increased radiation pressure which has a strong effect on the inner disc, blowing away the outer layers (farthest from the orbital plane). It is not appropriate to discuss our model in relation to QPO in detail here, however, we note that the blowing away is not inconsistent with the formation of QPO in the inner disc. It has been suggested that the upper kHz QPO frequency may correspond to a Keplerian frequency in the inner disc (e.g. Jonker et al. 2000). The removal of the outer parts of the inner disc by radiation pressure but not parts close to the orbital plane is not inconsistent with this, and it may even be that the disturbance to the disc triggers the oscillation.

4.1. The reduction in blackbody radius

Church & Bałucińska-Church (2001) can suggest why the neutron star blackbody emitting area decreases on the normal and horizontal branches. It is unlikely that this is due to any process on the stellar surface, and is more likely to be due to processes at the inner disc. In our survey of 14 LMXBs using *ASCA* and

BeppoSAX, we investigated the variation of blackbody luminosity with total luminosity. It is well-known that the blackbody fraction is small in faint sources rising to about 50% in sources close to the Eddington limit. The results were presented geometrically in terms of h, the half-height of the blackbody emitter, and H, the half-height of the inner disc. The blackbody luminosity depends on h, and is calculated from the blackbody radius (Sect. 3.2.1) while H is proportional to the mass accretion rate in the standard theory of the inner, radiatively-supported, disc (Frank et al. 2002). It was found that for all sources $h \simeq H$, suggesting that the neutron star emitting area was determined by the height of the inner disc. The mechanism for this might be radial flow across the gap between disc and neutron star, or alternatively the mechanism of Inogamov & Sunyaev (1999) which predicts that the accretion flow spreads vertically on the star to a height depending on $\dot{M}$. The survey results agreed approximately with this model (Church et al. 2002).

In a radiatively-supported disc, the vertical height of the disc increases rapidly with radial distance until at ∼10 km from the surface of the neutron star, it has its equilibrium value $H_{\rm eq}$ (Frank et al. 2002). In the present work on GX 340+0, $H_{\rm eq}$ calculated from the source luminosity varies between 30 km at the soft apex and 50 km at the hard apex, so that the inner disc towers above the neutron star. If the radiation pressure of the neutron star is strong, we would expect some of the inner disc to be blown away above and below the disc, leaving a residual inner disc of reduced height. On the basis of the survey results, the height on the neutron star would respond to this by becoming much smaller which may explain h decreasing from ∼11 km at the soft apex (where the radiation pressure is small) to ∼1 km on the horizontal branch.

4.2. The nature of the horizontal branch

The spectral fitting results show that the luminosity of the Comptonized emission increases on the normal branch and then decreases by about the same amount on the horizontal branch, following the same path in Fig. 5, suggesting that the mass accretion rate first increases, then decreases towards the initial value and we might expect the changes on the neutron star to also reverse at the hard apex. But the neutron star blackbody does not reverse its behaviour at the hard apex, the temperature and radius changing monotonically on the NB and HB (Fig. 4). A possible reason that this does not happen could relate to time delays in the system. An increase in $\dot{M}$ will affect the emission of the extended ADC first causing the source to move along the NB towards the hard apex, but changes in the blackbody emission would be delayed until the increase reaches the neutron star. Figure 4 provides evidence for this: the Comptonized emission has increased before the blackbody changes; Fig. 1 shows that several hours are required for the source to move halfway along the NB from the soft apex. This timescale is approximately consistent with estimates of flow times through the disc based on the viscous timescale (Frank et al. 2002). When $\dot{M}$ decreases in the disc then $L_{\rm ADC}$ falls, but the increase of $\dot{M}$ at the neutron star could continue for some time.

We next ask how the source leaves the HB end of the Z-track. Assuming as above that $\dot{M}$ has already decreased, we would expect the neutron star to cool, radiation pressure to fall and $R_{\rm BB}$ to increase. However, the effects in the ADC are not clear. If there was no change in the emission (as $\dot{M}$ is constant), the total luminosity would be about constant and the source may be able to jump from the HB to the NB as the neutron star cools. However, jumps have not so far been detected, and Z-track sources are seen to move smoothly from HB to NB.

We can assume that the X-ray luminosity is a good indicator of $\dot{M}$ when the radiation pressure is low (on the NB), but this is probably not true when the radiation pressure is high, so that the decreasing $L_{\rm CPL}$ on the HB may not mean that $\dot{M}$ falls. Firstly, the blowing away of outer layers of the inner disc by increased radiation pressure may reduce the ADC emission by a geometric factor (giving a reduction in $L_{\rm CPL}$) while $\dot{M}$ is constant or rising. In addition, the radiation pressure can divert a substantial fraction of $\dot{M}$ into the jets causing a decrease of $L_{\rm CPL}$ on the HB because of a decrease of accretion flow in the disc below the corona, reducing the electron density while the total $\dot{M}$, including the part diverted to the jets, remains constant, or increases. Then the asymmetry between the blackbody and Comptonized emission disappears, since the reversal of behaviour of both components takes place at the end of the Z-track, both components reversing their evolution when the mass accretion rate falls, the source moving back along the Z.

4.3. The nature of the flaring branch

We have suggested that on the flaring branch there is unstable nuclear burning. This is not unexpected since the theory of unstable nuclear burning (e.g. Bildsten 1998) shows that He burning in a hydrogen-rich environment should be unstable for $\dot{M} < 2.6 \times 10^{-8}\ M_{\odot}\,{\rm y}^{-1}$, while for higher $\dot{M}$, burning is stable. The Z-track sources have luminosities at about the Eddington limit, but lack of spectral fitting has often not allowed a definitive statement to be made on whether unstable burning is expected. However, Bildsten (1995) argued that the timescale of flaring in Sco X-1 is consistent with the timescale at which unstable burning starting in one part of the neutron star will spread across the surface. In sources of luminosity mid-way between burst sources and Z-track sources, we have previously detected bursting and flaring in the same observation, as in XB 1254-690 (Smale et al. 2002).

On the flaring branch, the blackbody radius increases systematically from its value of 10.8 ± 1.0 km at the soft apex to ∼16.1 ± 0.8 km. If we accept that the whole neutron star is emitting at the soft apex, then in flaring the emission must extend beyond the surface of the star. Similar values of $R_{\rm BB}$ greater than the neutron star radius have been found previously for Z-track sources, such as a value of 27 km found by Christian & Swank (1997) for GX 5-1. Lower luminosity X-ray burst sources can exhibit radius expansion (Lewin et al. 1985) in which $R_{\rm BB}$ increases indicating photospheric expansion due to radiation pressure, the luminosity remaining close to the Eddington limit. In the present work we also have an increase of $R_{\rm BB}$ on the flaring branch which we suggest is unstable nuclear burning, and the emitted flux approaches the Eddington flux. Thus it is possible that radius expansion may take place during flaring in the Z-track sources. The implication is that the emission expands beyond the surface of the neutron star, and the deep hole where the height of the inner accretion disc falls to that of the neutron star is partly filled by plasma. The rise in blackbody temperature is however, only 10%, and so much less than the temperature rise in X-ray bursts.

We next ask whether unstable nuclear burning takes place on all branches of the Z-track or only on the flaring branch. Conditions on the other branches either prevent unstable burning, or mask the appearance of flaring. On the flaring branch flares develop from the lowest X-ray intensity of the source at the soft apex, and are very obviously seen in the lightcurve. We

have examined the lightcurve for variations on timescales of a few thousand seconds in the other branches, but this was inconclusive. However, the present results suggest why unstable burning may occur only on the FB.

At the soft apex, $L_{\rm Tot}$ has its smallest value of 3.7×10^{38} erg s^{-1}, corresponding to a mass accretion rate per unit area on the neutron star $\dot{m} = 1.5 \times 10^5$ g cm^{-2} s^{-1}. The upper limit for unstable nuclear burning is $\dot{m} = 1.3 \times 10^5$ g cm^{-2} s^{-1} (Bildsten 1998). Thus the actual $\dot{m}$ is close to the theoretical upper limit which Bildsten estimates to be accurate to within 30%, and unstable burning can be possible. On the normal branch, the luminosity and mass accretion rate eventually approach a factor of 2 higher than at the soft apex suggesting that unstable burning is not possible and that flaring will not take place on the NB and HB. On the flaring branch, the emitting blackbody area increases, and so $\dot{m}$ remains below the critical value, and nuclear burning remains unstable. Examination of the lightcurve (Fig. 1) shows that flaring begins *exactly* at the lowest luminosity of the source. Thus if we move towards the soft apex along the NB, it may be that unstable burning begins immediately $\dot{m}$ falls below the critical value. Thus the identification of the flaring branch with unstable nuclear burning appears to be consistent with theory, as is the lack of unstable nuclear burning on the NB and HB.

4.4. The formation of jets by radiation pressure

Explaining the formation of relativistic jets from the neighbourhood of compact objects in both Galactic sources and in AGN has been a major astrophysical goal. Two main types of model have been proposed. First, it has long been suspected that radiation pressure may play an important role (Begelman & Rees 1984), and Lynden-Bell (1978) suggested that a radiatively-thickened inner accretion disc will define two funnels which allow jet formation perpendicular to the disc, driven by radiation pressure. Second, the other type of model depends on electromagnetic production via strong electric fields arising from magnetic fields in the disc around a black hole (Blandford & Znayek 1977). The present work reveals the link between jet formation and the position on the Z-track where the radiation pressure is high, strongly indicating the importance of radiation pressure.

It is well known that radio emission is detected from Z-track sources on the horizontal branch, and upper normal branch providing strong evidence that jets are present. On this part of the Z-track the high neutron star temperatures we determine mean that the radiation pressure of the neutron star is high, the emitted flux approaching three times super-Eddington (Fig. 7). It thus appears significant that jets are formed on this part of the Z-track suggesting that the launching of jets is due to the strong radiation pressure. Our spectral fitting result that the emitting area on the neutron star decreases is consistent with matter being blown away from the inner disc, and the release of matter within the system is directly supported by the measured increase of column density to a maximum at the hard apex. We thus propose that jets are formed by the very strong radiation pressure of the neutron star at this part of the Z-track, where the radiation flux substantially exceeds the Eddington flux. The emission area is small implying it is from an equatorial strip around the neutron star, and this geometry favours upwards direction of the jet. Radiation pressure acting horizontally may disturb the inner disc. However, a line from the equatorial belt to the inner edge of the disc will rise steeply upwards, the radiation pressure acting in a direction approaching vertical.

Jets are not seen on the flaring branch, and this is consistent with the model proposed. The radiation pressure is not so strong and the blackbody emitter apparently expands beyond the neutron star surface. There is normally a conical funnel in the central radiatively-supported inner accretion disc (Frank et al. 2002) where the disc height falls rapidly towards the stellar surface providing an opening for jet formation on the NB and HB. However, in flaring this funnel may be partly or completely blocked by plasma this also opposing jet formation.

Acknowledgements. This work was supported in part by the Polish KBN grant KBN-1528/P03/2003/25 and by PPARC grant PPA/G/S/2001/00052. We thank the referee for his very useful comments.

References

Agrawal, V. K., & Sreekumar, P. 2003, MNRAS, 346, 933
Bałucińska-Church, M., & Church, M. J. 2005, Proc of Interacting Binaries: Accretion, Evolution and Outcomes, Cefalu, July 2004, AIP Conf Proc, New York, 797, 339
Bałucińska-Church, M., Church, M. J., Oosterbroek, T., et al. 1999, A&A, 349, 495
Bałucińska-Church, M., Humphrey, P. J., Church, M. J., & Parmar, A. N. 2000, A&A, 360, 583
Bałucińska-Church, M., Barnard, R., Church, M. J., & Smale, A. P. 2001, A&A, 378, 847
Barnard, R., Bałucińska-Church, M., Smale, A. P., & Church, M. J. 2001, A&A, 380, 494
Barnard, R., Church, M. J., & Bałucińska-Church, M. 2003, A&A, 405, 237
Begelman, M. C., & Rees, M. J. 1984, MNRAS, 206, 209
Bildsten, L. 1995, ApJ, 438, 852
Bildsten, L. 1998, in The Many Faces of Neutron Stars, ed R. Buccheri, J. van Paradijs, & M. A. Alpar, Proc NATO ASIC 515 (Dordrecht: Kluwer), 419
Blandford, R. D., & Znayek, R. L. 1977, 179, 433
Bradshaw, C. F., Geldzahler, B. J., & Fomalont, E. B. 2003, ApJ, 592, 486
Church, M. J. 2001, Adv Space Res, 28, 323
Church, M. J., & Bałucińska-Church, M. 1995, A&A, 300, 441
Church, M. J., & Bałucińska-Church, M. 2001, A&A, 369, 915
Church, M. J., & Bałucińska-Church, M. 2004, MNRAS, 348, 955
Church, M. J., Mitsuda, K., Dotani, T., et al. 1997, ApJ, 491, 388
Church, M. J., Bałucińska-Church, M., Dotani, T., & Asai, K. 1998a, ApJ, 504, 516
Church, M. J., Parmar, A. N., Bałucińska-Church, M., et al. 1998b, A&A, 338, 556
Church, M. J., Inogamov, N. A., & Bałucińska-Church, M. 2002, A&A, 390, 139
Church, M. J., Reed, D., Dotani, T., Bałucińska-Church, M., & Smale, A. P. 2005, 359, 1336
Christian, D. J., & Swank, J. H. 1997, ApJS, 109, 177
Dickey, J. M., & Lockman, F. J. 1990, ARA&A, 28, 215
di Salvo, T., & Stella, L. 2002, in Proc of XXII Moriond astrophysics meeting: The Gamma-ray Universe, ed. A. Goldwurm, D. Neumann, & J. Tran Than Van, Les Arcs, March 2002 (Vietnam: the Gioi Publishers)
di Salvo, T., Stella, L., Robba, N. R., et al. 2000, ApJ, 544, L119
di Salvo, T., Robba, N. R., Iaria, R., et al. 2001, ApJ, 554, 49
di Salvo, T., Farinelli, R., Burderi, L., et al. 2002, A&A, 386, 535
Done, C., Życki, P., & Smith, D. A. 2002, MNRAS, 331, 453
Fender, R. P., & Hendry, M. A. 2000, MNRAS, 317, 1
Frank, J., King, A. R., & Raine, D. J. 2002, Accretion Power in Astrophysics, third edition (Cambridge University Press)
Fujimoto, M. Y., Hanawa, T., & Miyaji, S. 1981, ApJ, 247, 267
Fushiki, I., & Lamb, D. Q. 1987, ApJ, 323, L55
Hasinger, G., & van der Klis, M. 1989, A&A, 225, 79
Hasinger, G., Priedhorsky, W., & Middleditch, J. 1989, ApJ, 337, 843
Hasinger, G., van der Klis, M., Ebisawa, K., Dotani, T., & Mitsuda, K. 1990, A&A, 235, 131
Inogamov, N. A., & Sunyaev, R. A. 1999, AstL, 25, 269
Jahoda, K., Swank, J. H., Giles, A. B., et al. 1996, SPIE, 2808, 59
Jonker, P. G., Wijnands, R., van der Klis, M., et al. 1998, ApJ, 499, L191
Jonker, P. G., van der Klis, M., Wijnands, R., et al. 2000, ApJ, 537, 374
Kahn, S. M., & Grindlay, J. E. 1984, ApJ, 281, 826
Kuulkers, E., van der Klis, M., Oosterbroek, T., et al. 1994, A&A, 289, 759
Kuulkers, E., van der Klis, M., & van Paradijs, J. 1995, ApJ, 450, 748
Kuulkers, E., van der Klis, M., Oosterbroek, T., van Paradijs, J., & Lewin, W. H. G. 1997, MNRAS, 287, 495

Kuulkers, E., Homan, J., van der Klis, M., Lewin, W. H. G., & Mendéz, M. 2002, A&A, 382, 947
Lewin, W. H. G., van Paradijs, J., & Taam, R. E. 1995, in X-ray Binaries, ed. W. H. G. Lewin, J. van Paradijs, & E. P. J. van den Heuvel (Cambridge University Press)
Lynden-Bell, D. 1978, Phys Scripta, 17, 185
Makishima, K. 1986, The Physics of Accretion onto Compact Objects, Proc. of Tenerife workshop, 1986 (Springer-Verlag), Lect. Not. Phys., 266, 249
Migliari, S., & Fender, R. P. 2006, MNRAS, 366, 79
Mitsuda, K., Inoue, H., Nakamura, N., & Tanaka, Y. 1989, PASJ, 41, 97
Penninx, W. 1989, in Proceedings of the 23rd ESLAB Symposium on Two Topics in X-ray Astronomy, ed. J. Hunt, & B. Battrick, Bologna, Sept. 1989 (ESA publications), ESA SP-296, 185
Penninx, W., Lewin, W. H. G., Tan, J., et al. 1991, MNRAS, 249, 113
Penninx, W., Zwarthoed, G. A. A., van Paradijs, J., et al. 1993, A&A, 267, 92
Petrucci, P. O., Haardt, F., Maraschi, L., et al. 2001, ApJ, 556, 716
Priedhorsky, W., Hasinger, G., Lewin, W. H. G., et al. 1986, ApJ, 306, L91
Psaltis, D., Lamb, F. K., & Miller, G. S. 1995, ApJ, 454, L137
Schatz, H., Bildsten, L., Cumming, A., & Wiescher, M. 1999, ApJ, 524, 1014
Schulz, N. S., & Wijers, R. A. M. J. 1993, A&A, 273, 123
Schulz, N. S., Hasinger, G., & Trümper, J. 1989, A&A, 225, 48
Shapiro, S. L., Lightman, A. P., & Eardley, D. M. 1976, ApJ, 204, 187
Smale, A. P. 1998, ApJ, 498, L141
Smale, A. P., Church, M. J., & Bałucińska-Church, M. 2001, ApJ, 550, 962
Smale, A. P., Church, M. J., & Bałucińska-Church, M. 2002, ApJ, 581, 1286
Sztajno, M., van Paradijs, J., Lewin, W. H. G., et al. 1986, MNRAS, 222, 499
Tawara, Y., Hirano, T., Kii, T., Matsuoka, M., & Murakami, T. 1984, PASJ, 36, 861
Titarchuk, L. 1994, ApJ, 434, 313
van der Klis, M., Stella, L., White, N. E., Jansen, F., & Parmar, A. N. 1987, ApJ, 316, 411
van Paradijs, J., Hasinger, G., Lewin, W. H. G., et al. 1988, MNRAS, 231, 379
van Paradijs, J., Allington-Smith, J., Callanan, P., et al. 1990, A&A, 235, 156
Vrtilek, S. D., Raymond, J. C., Garcia, M. R., et al. 1990, A&A, 235, 162
Wijnands, R. A. D., van der Klis, M., Kuulkers, E., Asai, K., & Hasinger, G. 1997, A&A, 323, 399
White, N. E., Peacock, A., Hasinger, G., et al. 1986, MNRAS, 218, 129